JSHC
Japan Society of Histochemistry and Cytochemistry
Established 1959

Acta Histochem. Cytochem. 39 (5): 125–138, 2006
doi:10.1267/ahc.06008

Calcium-binding Protein Calretinin Immunoreactivity in the Dog Superior Colliculus

Jea-Young Lee[1], Jae-Sik Choi[1], Chang-Hyun Ahn[1], In-Suk Kim[2], Ji-Hong Ha[3] and Chang-Jin Jeon[1]

Department of [1]Biology and [3]Genetic Engineering, College of Natural Sciences, Kyungpook National University, Daegu, 702–701 and [2]Department of Ophthalmic Optics, Chodang University, Muan, Jeonnam Province, 534–701, Korea

Received March 20, 2006; accepted August 4, 2006; published online September 27, 2006

We studied calretinin-immunoreactive (IR) fibers and cells in the canine superior colliculus (SC) and studied the distribution and effect of enucleation on the distribution of this protein. Localization of calretinin was immunocytochemically observed. A dense plexus of anti-calretinin-IR fibers was found within the upper part of the superficial gray layer (SGL). Almost all of the labeled fibers were small in diameter with few varicosities. The intermediate and deep layers contained many calretinin-IR neurons. Labeled neurons within the intermediate gray layer (IGL) formed clusters in many sections. By contrast, labeled neurons in the deep gray layer (DGL) did not form clusters. Calretinin-IR neurons in the IGL and DGL varied in morphology and included round/oval, vertical fusiform, stellate, and horizontal neurons. Neurons with varicose dendrites were also labeled in the IGL. Most of the labeled neurons were small to medium in size. Monocular enucleation produced an almost complete reduction of calretinin-IR fibers in the SC contralateral to the enucleation. However, many calretinin-IR cells appeared in the contralateral superficial SC. Enucleation appeared to have no effect on the distribution of calretinin-IR neurons in the contralateral intermediate and deep layers of the SC. The calretinin-IR neurons in the superficial dog SC were heterogeneous small- to medium-sized neurons including round/oval, vertical fusiform, stellate, pyriform, and horizontal in shape. Two-color immunofluorescence revealed that no cells in the dog SC expressed both calretinin and GABA. Many horseradish peroxidase (HRP)-labeled retinal ganglion cells were seen after injections into the superficial layers. The vast majority of the double-labeled cells (HRP and calretinin) were small cells. The present results indicate that antibody to calretinin labels subpopulations of neurons in the dog SC, which do not express GABA. The results also suggest that the calretinin-IR afferents in the superficial layers of the dog SC originate from small class retinal ganglion cells. The expression of calretinin might be changed by the cellular activity of selective superficial collicular neurons. These results are valuable in delineating the basic neurochemical architecture of the dog visual system.

Key words: calretinin, enucleation, localization, superior colliculus

I. Introduction

Calcium-binding proteins have been demonstrated to facilitate as good markers to distinguish subpopulations of neurons [2, 4]. These proteins also have been implicated in many studies because their distribution changes in many neurodegenerative disorders [12, 24, 43]. Among the many calcium-binding proteins, three calcium-binding proteins in particular, calbindin D28K, calretinin, and parvalbumin, abundantly occur in various types of neurons in the central nervous system [2, 4, 11, 41]. However, the functions of these proteins have not been established. They may simply work as calcium buffers, or they may actively work in calcium-mediated signal transduction [40, 43].

The mammalian superior colliculus (SC) is a highly

Correspondence to: Prof. Chang-Jin Jeon, Ph.D., Department of Biology, College of Natural Sciences, Kyungpook National University, 1370 Sankyuk-dong, Daegu, 702–701, S. Korea.
E-mail: cjjeon@knu.ac.kr

differentiated region of alternating fibers and cells lying on the roof of the midbrain and is the center of visuo-motor integration. It is a seven-layered structure that can be divided into three superficial (zonal, ZL; superficial gray, SGL; and optic layers, OL) and four deep layers (intermediate gray, IGL; intermediate white, IWL; deep gray, DGL; and deep white layers, DWL) [10, 14]. One of the principal organizing features of the SC is the topographical distribution of its afferents and efferents. Many afferent fibers and efferent cells are segregated into specific laminae or have puffs and patches that were first described by Graybiel [10, 14, 15, 17]. Calcium-binding proteins exhibit horizontal laminar segregation in the SC. Thus, the calcium-binding protein calbindin D28K is found in cells that are located in three layers of the mammalian SC [3, 23, 29, 31, 44]. The parvalbumin-immunoreactive (IR) neurons are concentrated in a dense tier within the deep SGL and upper OL [5, 32]. Calretinin forms a dense plexus of immunoreactive fibers in the superficial layers of the SC [8, 13, 21, 23, 42, 46]. However, there are significant differences in the distribution of calretinin in the rabbit SC [20].

We have previously reported the distribution of calretinin in visual system of several lower mammalian SCs [13, 20, 21, 50]. However, direct application of data obtained in lower animals to humans is limited as the physiology of lower animals is profoundly different from that of humans. The degree of pathological and genetic features of dogs is very close to humans [38]. However, calcium-binding protein calretinin immunoreactivity has not been reported in the dog SC. Thus, the main purpose of the present study was to provide infrastructural knowledge of calretinin chemoarchitecture in the dog SC by analyzing the morphology, distribution, and effect of enucleation, as dogs are an integral part of the research process [22, 38, 49]. Our understanding of how the human brain functions in health and disease will benefit from comparison of its structure with the brain of the dog. Our secondary purpose was to investigate whether there are any species differences in the distribution of this protein, as various species are used in anatomical and physiological studies of collicular neurotransmission.

II. Materials and Methods

Animals

Twelve Korean natural dogs (Three Sapsarees and nine Korean mixed breed dogs; 4–12 months, 4–10 kg) were used for these experiments. The Sapasrees were obtained from a breeding colony maintained by the Foundation for Sapsaree Conservation in Daegu, Korea and the mixed-breed dogs were obtained from a local vendor. The animals were divided into three groups. First, intact dogs (n=4; two Sapsarees and two mixed-breed dogs) were used to determine the normal distribution of immunoreactivity to the calcium-binding protein calretinin. Second, unilaterally enucleated dogs (n=2; one Sapsaree and one mixed-breed dog) were produced in order to examine the effects of retinal differentiation. Third, horseradish peroxidase (HRP) was used (n=6; mixed-breed dogs) as a retrograde tracer to identify neurons in the retina which project to SC. Enucleation was performed under deep anesthesia with a mixture of ketamine hydrochloride (30–40 mg/kg) and xylazine (3–6 mg/kg) (supplemented as needed to maintain anesthesia). Proparacaine HCl (200–300 μl) was applied to the cornea to suppress blink reflexes. The eyes were removed by carefully cutting the extrinsic muscles and connective tissue surrounding the eyeball, and finally severing the optic nerve just behind the optic disc. The wound was then filled with sterile gelform to prevent bleeding. The animals were allowed to recover from the anesthetic under the warmth of an illuminated 100 W lamp. Intramuscular injection of a long-acting antiphlogistic Voren suspension (200–300 μl/kg, Boehringer Ingelheim Vetmedica Korea Ltd, Seoul, Korea) was given every four days. The enucleated dogs were allowed to survive for 10d. The National Institute of Health guidelines for the use and care of animals were followed for all experimental procedures. All efforts were made to minimize animal suffering as well as the number of animals used.

Perfusion and tissue processing

Dogs were anesthetized deeply with a mixture of ketamine hydrochloride (30–40 mg/kg) and xylazine (3–6 mg/kg) before perfusion. All dogs were perfused intracardially with 4% paraformaldehyde and 0.3–0.5% glutaraldehyde in 0.1 M sodium phosphate buffer (pH=7.4) with 0.002% calcium chloride added. After exposure of the thoracic cavity, 1% sodium nitrite (0.3 ml/kg) and 25,000 units of sodium heparin (0.5 ml/kg) were injected directly into the heart to dilate the blood vessels and reduce coagulation. Following a prerinse with of phosphate-buffered saline (PBS, pH=7.2, approximately 500 ml/kg) over a period of 3–4 min, each dog was perfused with the same fixative (approximately 1000 ml/kg) for 1–2 hr via a syringe needle inserted through the left ventricle and aorta. The head was then removed and placed in the fixative for 2–3 hr. The brain was then removed from the skull and stored 2–3 hr in the same fixative and left overnight in 0.1 M phosphate buffer (pH=7.4) containing 8% sucrose and 0.002% $CaCl_2$. The SC was removed, mounted onto a chuck, and cut into 50 μm thick coronal sections with a vibratome.

HRP immunocytochemistry

A polyclonal antibody against calretinin (Chemicon, USA) and a monoclonal antibody against GABA (Sigma, USA) were used in the present study. The SC sections were processed free floating in small vials. For immunocytochemistry, the sections were incubated in 1% sodium borohydride ($NaBH_4$) for 30 min. Subsequently, these sections were rinsed for 3×10 min in 0.25 M Tris buffer, and then incubated in 0.25 M Tris buffer with 4% normal serum (normal goat serum for calretinin and normal horse serum for GABA) for 2 hr with 0.5% Triton X-100 added. The sections were then incubated in the primary antiserum in 0.25 M Tris buffer with 4% normal serum for 48 hr with 0.5% Triton X-100 added. The primary antibody was diluted

1:500–1000 (calretinin) or 1:100–200 (GABA). Following 3×10 min rinses in 0.25 M Tris buffer, the sections were incubated in a 1:200 dilution of biotinylated secondary IgG in 0.25 M Tris buffer with 4% normal serum for 2 hr with 0.5% Triton X-100 added. The sections were then rinsed for 3×10 min in 0.25 M Tris buffer and then incubated in a 1:50 dilution of avidin-biotinylated horseradish peroxidase complex (Vector lab, USA) in 0.25 M Tris buffer for 2 hr. The sections were again rinsed in 0.25 M Tris buffer for 3×10 min. Finally, the staining was visualized by reacting with 3,3'-diaminobenzidine tetrahydrochloride (DAB) and hydrogen peroxide in 0.25 M Tris buffer for 3–10 min using a DAB reagent set (Kirkegaard & Perry, USA). All sections were then rinsed in 0.25 M Tris buffer before mounting. Retinal whole mounts were processed longer than vibratome sections to achieve complete penetration of antibodies using the standard whole-mount immunocytochemical techniques [20]. They were processed 72 hr in the primary antibody and 24 hr in the secondary antibody and ABC complex, respectively. As a control, some sections were incubated in the same solution without adding the primary antibody. These control tissues showed no calretinin immunoreactivity. Following the immunocytochemical procedures, the tissue was mounted on Superfrost Plus slides (Fisher, USA) and dried overnight in a 37°C oven. Then mounted sections were dehydrated, cleared, and coverslipped. Some whole mounts were coverslipped in glycerol without the dehydration procedures. The tissues were examined and photographed with a Zeiss Axioplan microscope, using conventional or differential interference contrast (DIC) optics.

Fluorescence immunocytochemistry

To generate two simultaneous labels, the sections were incubated in the primary antiserum using the appropriate steps described above. For detection by immunofluorescence, the secondary antibodies were fluorescein-conjugated anti-rabbit IgG (Vector lab) for detecting the anti-calretinin antibody and Cy5-conjugated anti-mouse IgG (Jackson ImmunoResearch Lab.) for detecting the anti-GABA antibody. Labeled sections were coverslipped with Vectashield mounting medium (Vector lab). Images were obtained and viewed with a Zeiss LSM510 laser scanning confocal microscope.

Injection of horseradish peroxidase (HRP)

HRP (Sigma, Type IV) was used for experiments designed to label retinotectal projection neurons. Injections into the superficial layers of the SC were made in six dogs. Substantial retrograde labeling of ganglion cells with HRP was obtained in two animals in which we had successfully injected superficial SC. A 5 μl Hamilton microsyringe with a 30 gauge needle mounted on a specially designed injection device attached to the stereotaxic apparatus was used to inject the HRP solution. Injections consisted of 0.3–1.5 μl of a 30% HRP solution in distilled water. Animals were then allowed to recover and to survive for 48 hr before perfusion.

HRP histochemistry

Retrogradely transported HRP was identified by a previously described, cobalt-nickel intensification procedure [35]. Briefly, the tissue sections were incubated in a solution of 0.05% diaminobenzidine tetrahydrochloride with 0.005% nickel chloride and 0.005% cobalt acetate in 0.1 M phosphate buffer for 10 min, and further incubated in 0.05% DAB with 0.01% hydrogen peroxidase (H_2O_2) for 15–30 min. The sections were then rinsed several times in PBS before being reacted for immunocytochemistry.

Data analysis

To determine the morphological types of the calretinin-IR cells, we sampled from five sequential fields, each 310 μm×310 μm in area, across the SGL, IGL, and DGL of the SC. Each field was positioned at approximately equal intervals. Large blood vessels were excluded from the measurement fields by moving the field slightly to avoid biasing the measures. Analysis was done with a 40× Zeiss Plan-Apochromat objective. Cell types within the IGL and DGL were analyzed from the three (one rostral, one middle, and one caudal SC) best labeled sections from each of two normal animals (total 30 fields in each layer). Cell types within the SGL were analyzed from the three (one rostral, one middle, and one caudal SC) best labeled sections from each of two enucleated animals (total 30 fields). To obtain the best images, we analyzed the cells under differential interference contrast (DIC) optics. Only cell profiles containing a nucleus and at least a faintly visible nucleolus were included for analysis. The goal of the present study was to obtain an estimate of each morphological cell type.

To compare the number of calretinin-IR cells of the normal SC, and the ipsilateral and contralateral sides of the enucleated dogs, we also counted the labeled cells in five sequential fields, each 500 μm×500 μm in area, across the medial-lateral extent of the SC. Each field was centered over the SGL, IGL, and DGL. Three tissue sections (one rostral, one middle, and one caudal) from the four normal and two enucleated animals were measured. We summed the numbers of labeled cells obtained to compare the normal (total 60 fields in each layer from four normal SC), ipsilateral (total 30 fields in each layer from two enucleated dogs), and contralateral sides (total fields in each layer from the two enucleated dogs) to the enucleation. The number of calretinin-IR cells on the ipsilateral and contralateral sides to the enucleation was expressed as the percentage of the labeled cells on the normal control side. The ratios were evaluated statistically by a Student's *t*-test between the normal and ipsilateral, and contralateral sides to the enucleation.

III. Results

Distribution of calretinin immunoreactivity

Calretinin immunoreactivity was very selectively distributed in the SC of all normal dogs. A dense plexus of calretinin-immunoreactive (IR) fibers was found within the upper part of the SGL throughout the rostrocaudal extent

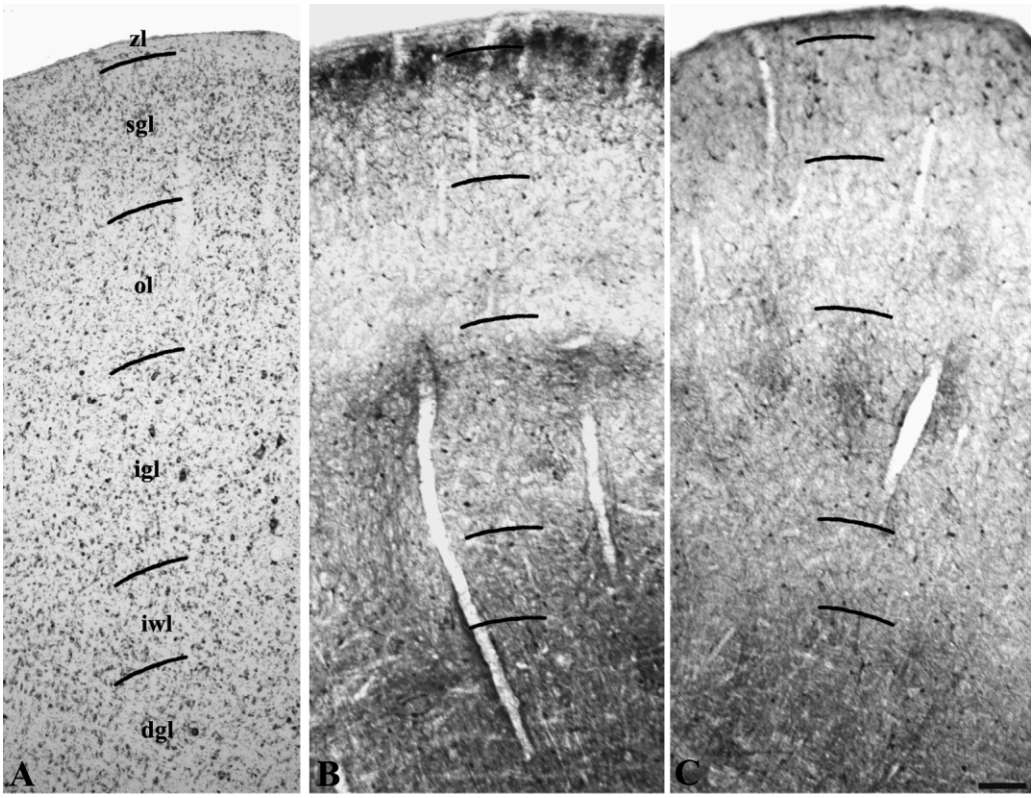

Fig. 1

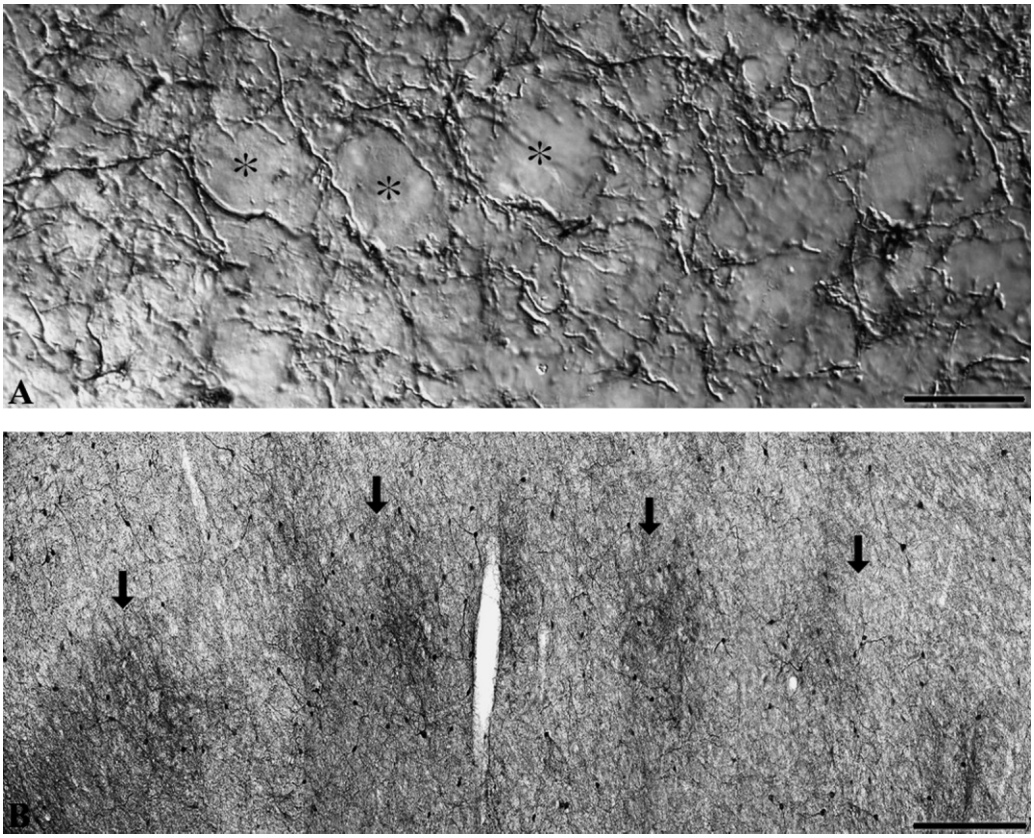

Fig. 2

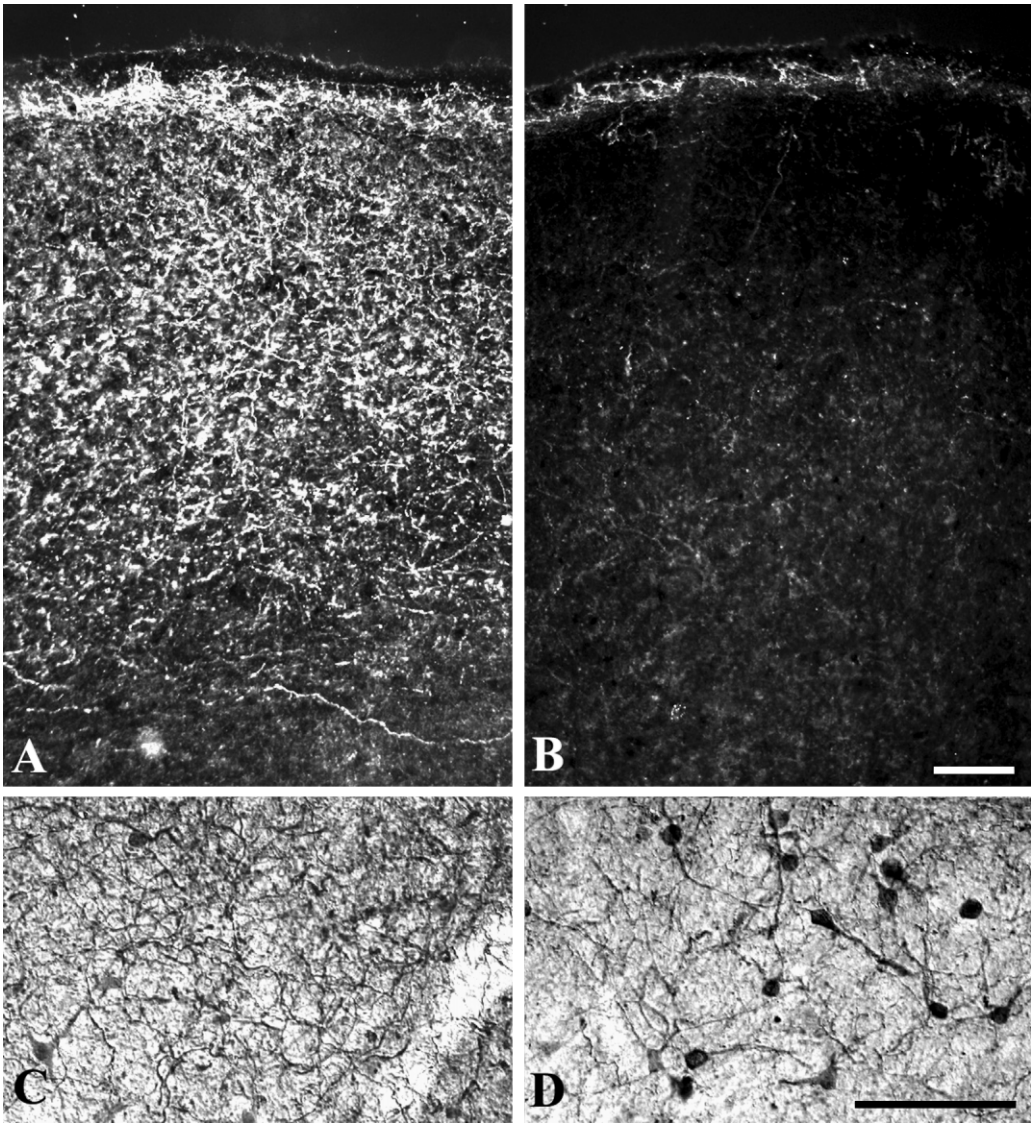

Fig. 3. Low magnification of dark-field (**A, B**) and bright-field (**C, D**) photomicrographs of calretinin-IR fibers and cells in the dog SC. (**A**) Calretinin-IR fibers were concentrated within the upper part of the SGL in normal SC. (**B**) Fiber staining was almost completely reduced in the side of SC contralateral to the enucleation. Low magnification bright-field photomicrographs from the SGL in the (**C**) normal and (**D**) contralateral SC to the enucleation. Note the new appearance of many calretinin-IR neurons after enucleation. Bar=100 μm.

(Figs. 1, 3); its thickness was approximately 400–500 μm at the middle level. This tier of labeled fibers was found throughout the rostral-caudal extent of the dog SC. Some calretinin-IR fibers were also found in the ZL. Calretinin-IR fibers gradually decreased in density in the lower part of the SGL and were only very sparsely distributed in the OL. All calretinin-IR fibers in the superficial layers were small in diameter with few varicosities (Figs. 2A, 3). No calretinin-

Fig. 1. Low power photomicrographs of the laminar distribution of calretinin-IR neurons in the dog SC. (**A**) Thionin-stained section showing collicular lamination. (**B**) Anti-calretinin-immunoreactivity in normal SC. Calretinin-IR fibers were distributed in the upper part of the superficial layers. The majority of calretinin-IR neurons were distributed in the IGL and DGL. Note the clusters of labeled neurons in the IGL. (**C**) Anti-calretinin-immunoreactivity in enucleated SC. The fiber staining was almost completely reduced in the side of SC contralateral to the enucleation. zl, zonal layer; sgl, superficial gray layer; ol, optic layer; igl, intermediate gray layer; iwl, intermediate white layer, dgl, deep gray layer. Bar=200 μm.

Fig. 2. (**A**) High magnification Nomarski differential interference contrast photomicrograph of calretinin-IR fibers in the SGL. Almost all of the labeled fibers are small with few varicosities. Note that the calretinin-IR fibers surround unlabeled cell somata (asterisks). (**B**) Medium magnification of calretinin-IR neurons in the IGL. Arrows indicate clustering of calretinin-IR neurons. Bar=20 μm (**A**) and 100 μm (**B**).

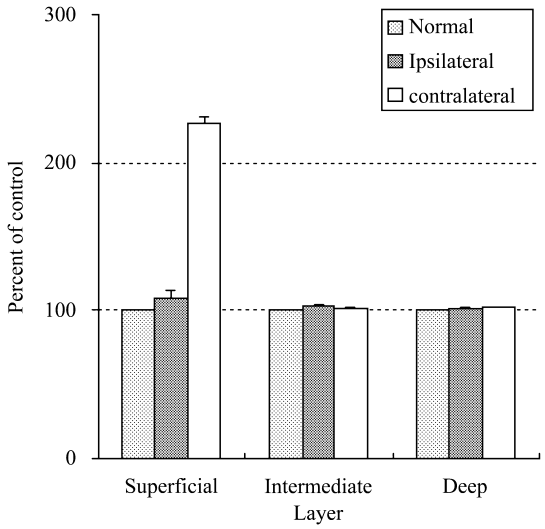

Fig. 4. The effects of monocular enucleation on the calretinin-IR neurons. In the normal SGL, 1046 calretinin-IR cells from 12 sections (mean±S.D.=261.50±10.75) of 4 normal dogs were counted. In the SGL of enucleated dogs, 566 (mean±S.D.=283±12.72) on the ipsilateral sides and 1184 (mean±S.D.=592±14.14) on the contralateral sides from 6 sections were counted. Calretinin-IR cells of the enucleated dogs increased 8.22% (p=0.09) on the ipsilateral SGL, 126.38% (p<0.0001) on the contralateral SGL. In the normal IGL, 2264 calretinin-IR cells from 12 sections (mean±S.D.=566±14.67) of 4 normal dogs were counted. In the IGL of enucleated dogs, 1169 (mean±S.D.=584.50±3.53) on the ipsilateral sides and 1144 (mean±S.D.=572±7.07) on the contralateral sides from 6 sections were counted. Calretinin-IR cells of enucleated dogs increased 3.26% (p=0.17) on the ipsilateral IGL, 1.06% (p=0.62) on the contralateral IGL. In the normal DGL, 2199 calretinin-IR cells from 12 sections (mean±S.D.=549.75±17.70) of 4 normal dogs were counted. In the DGL of enucleated dogs, 1117 (mean±S.D.=558.50±6.36) on the ipsilateral sides and 1120 (mean±S.D.=560±16.97) on the contralateral sides from 6 sections were counted. Calretinin-IR cells of the enucleated dogs increased 1.59% (p=0.55) on the ipsilateral DGL, 1.86% (p=0.53) on the contralateral DGL. Compared with the normal SC, enucleation caused an enormous increase of calretinin-IR neurons in the superficial layer, while there were almost no changes in the intermediate and deep layers. The results are expressed as percentages of the normal SC.

Table 1. *Changes in the number of calretinin-IR neurons in the dog SC after monocular enucleation*

SC sides	Animal No.	No. Sections	No. calretinin-IR neurons		
			SGL	IGL	DGL
Normal SC	SA1	3	251	580	556
	SA2	3	275	565	535
	MB1	3	255	573	572
	MB2	3	265	546	536
	Total	12	1046	2264	2199
	(Mean±S.D.)		261.5±10.75	566±14.67	549.75±17.70
Enucleated ipsilateral SC	SA3	3	292	582	563
	MB3	3	274	587	554
	Total	6	566	1169	1117
	(Mean±S.D.)		283±12.72	584.5±3.53	558.5±6.36
	% changes		8.22	3.26	1.59
Enucleated contralateral SC	SA3	3	582	577	548
	MB3	3	602	567	572
	Total	6	1184	1144	1120
	(Mean±S.D.)		592±14.14	572±7.07	560±16.97
	% changes		126.38	1.06	1.86

SA, Sapsaree; MB, mixed-breed.

IR large varicose fibers were found. The dense band of calretinin-IR fibers in the superficial layers contained some calretinin-IR cells. However, the majority of the calretinin-IR cells in the band were lightly labeled for calretinin (Fig. 3C). Some scattered neurons were localized in the OL (Fig. 1). In contrast to the superficial layers, intermediate and

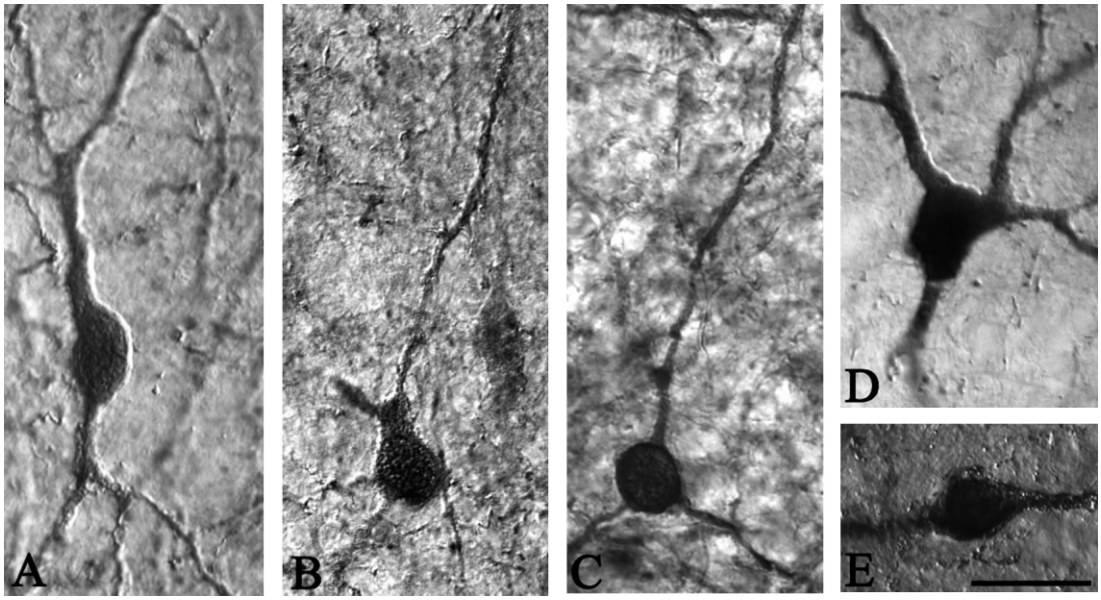

Fig. 5. High magnification of calretinin-IR neurons in the SGL contralateral to the enucleation. (**A**) A vertical fusiform neuron with proximal dendrite projecting superficially toward the pial surface. (**B**) A pyriform cell with a thick primary dendrite oriented toward the pial surface. (**C**) A small multipolar round cell. (**D**) A medium-sized multipolar stellate cell. (**E**) A horizontal cell with fusiform cell body and horizontally oriented dendrites. Bar=20 μm.

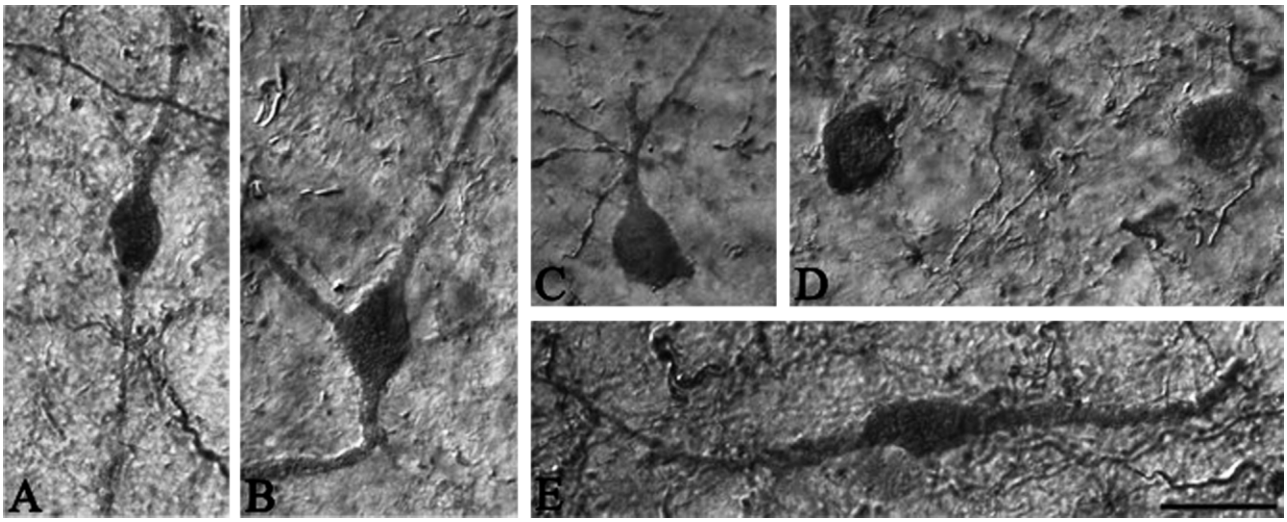

Fig. 6. High magnification of calretinin-IR neurons in the SGL of normal SC. (**A**) A vertical fusiform neuron with proximal dendrite projecting superficially toward the pial surface. (**B**) A medium-sized multipolar stellate cell. (**C**) A pyriform cell with a thick primary dendrite oriented toward the pial surface. (**D**) Small round/oval cells. (**E**) A horizontal cell with fusiform cell body and horizontally oriented dendrites. Bar= 20 μm.

deep layers contained many calretinin-IR neurons and showed a different distribution pattern. They formed two patterns in the SC. The first pattern, which was distinctive, was found in the IGL (Fig. 1). In many sections, calretinin-IR neurons in the IGL formed clusters of labeled neurons. These clusters were approximately 300–400 μm in diameter. Figure 2B (arrows) shows four calretinin-IR neuron clusters in the IGL. The second pattern of calretinin-IR neurons was found in the DGL. However, the second pattern was not distinctive compared to the first tier, and the labeled neurons did not form any clusters (Fig. 1). These neurons were scattered among the layers. Some scattered neurons were also observed in other layers. The calretinin-IR neurons in the IGL and DGL could be seen throughout the rostrocaudal extent of the SC.

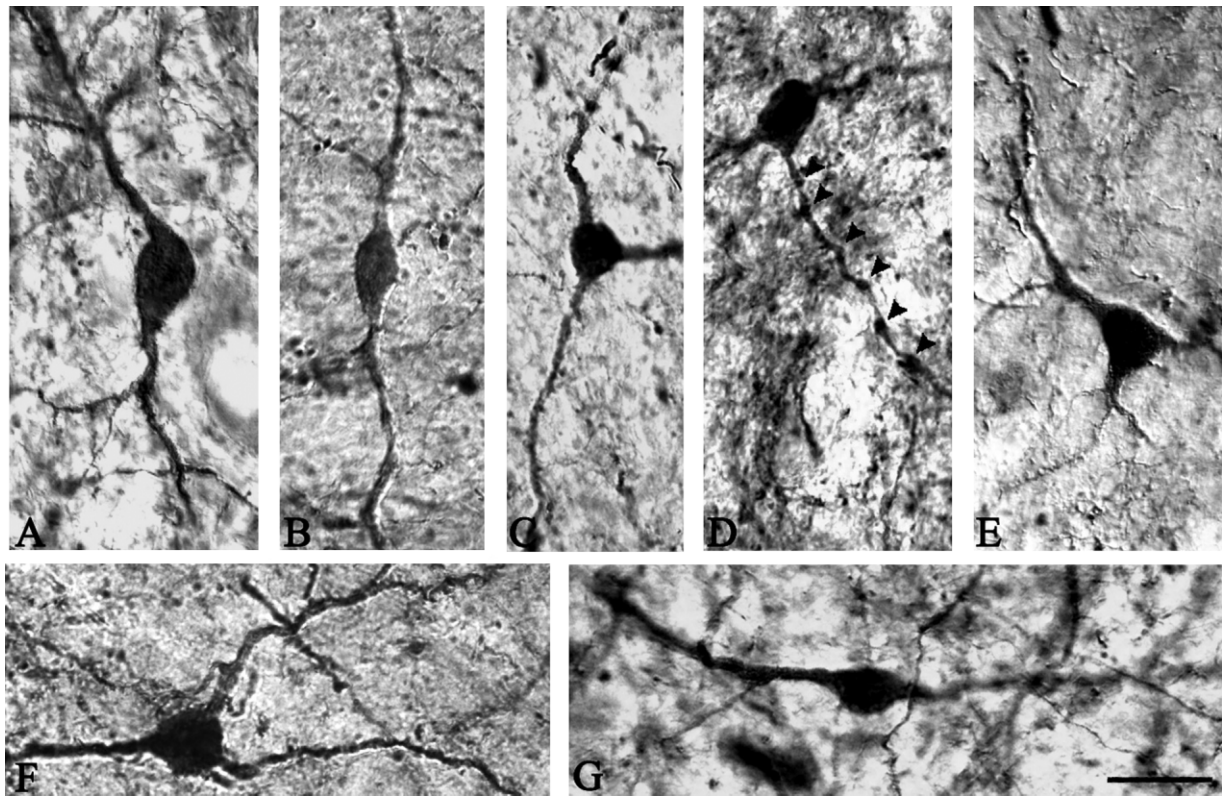

Fig. 7. High magnification Nomarski differential interference contrast photomicrographs of calretinin-IR neurons in the IGL of normal SC. (**A, B**) Vertical fusiform neurons with proximal dendrite projecting superficially toward the pial surface. (**C, F**) Small- to medium-sized multipolar round/oval cells. (**D**) Calretinin-IR neuron with varicose dendrites. The varicosities (arrowheads) often appeared at fairly regular intervals. (**E**) A medium-sized multipolar stellate cell. (**G**) A horizontal cell with fusiform cell body and horizontally oriented dendrites. Bar=20 μm.

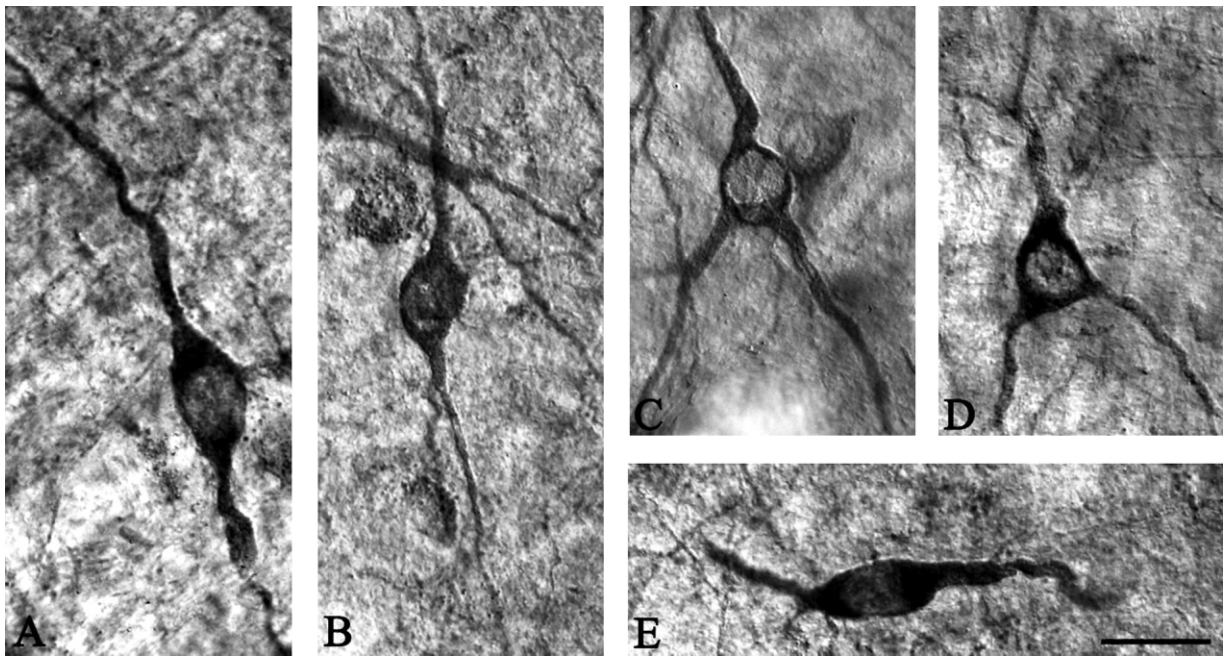

Fig. 8. High magnification Nomarski differential interference contrast photomicrographs of calretinin-IR neurons in the DGL normal SC. (**A, B**) Vertical fusiform neurons with proximal dendrite projecting superficially toward the pial surface. (**C**) A multipolar round neuron. (**D**) A multipolar stellate neuron. (**E**) A horizontal cell with fusiform cell body and horizontally oriented dendrites. Bar=20 μm.

Effects of monocular enucleation

To determine whether the calretinin-labeled fibers in the superficial layers originated from the retina and to investigate the activity-dependent changes of calretinin expression, we performed eye enucleation. Figure 1B (bright-field) and 3A (dark-field) show calretinin immunoreactivity in the normal dog SC, while Fig. 1C (bright-field) and 3B (dark-field) show calretinin immunoreactivity after monocular enucleation. A marked reduction of calretinin immunoreactivity was produced in the superficial layers of the SC contralateral to the enucleation; calretinin-positive fibers were almost completely eliminated following eye enucleation (Figs. 1C, 3B). By contrast, in the superficial layers of the SC contralateral to the enucleation, many calretinin-positive cells were observed (Figs. 1C, 3D). Enucleation appeared to have no effect on the distribution of calretinin-IR neurons in the contralateral IGL and DGL of the SC. Although we saw occasional variability in immunoreactivity in the contralateral and ipsilateral SC, there was no consistent difference after enucleation in labeled neurons on the two sides in calretinin-IR sections.

Quantitatively, after unilateral enucleation, there was a significant increase in the number of calretinin-IR cells on the contralateral experimental SGL compared to the normal SGL (Fig. 4). Calretinin-IR cells of the enucleated dogs increased in number; 8.22% ($p=0.09$) on the ipsilateral SGL, 126.38% ($p<0.0001$) on the contralateral SGL more numerous than those in the normal SGL. Unlike the SGL, after unilateral enucleation, there were no significant changes in the number of calretinin-IR cells on the ipsilateral and contralateral sides compared to the normal IGL and DGL (Table 1).

Morphology of calretinin-IR neurons

In the superficial layers of the SC contralateral to the enucleation, many calretinin-positive cells were newly observed. These cells were of various shapes; the principal neuronal type in the SGL labeled with antibody against calretinin was round or oval cells with many dendrites coursing in all directions. Figure 5C shows representative multipolar round or oval cells. Others were vertical fusiform, stellate, horizontal, and pyriform cells. Figure 5A shows a vertical fusiform cell that displays a vertical fusiform cell body with a main, long process ascending towards the pial surface and a long descending process. Figure 5D shows a medium-sized stellate neuron. Stellate cells had polygonally-shaped cell bodies with numerous dendrites coursing in all directions. Figure 5E shows a horizontal cell that displays a horizontally-oriented small, fusiform cell body and horizontally-oriented processes. The pyriform cells (Fig. 5B) had pear-shaped cell bodies and a thick, proximal dendritic stump directed superficially towards the pial surface. Pyriform and horizontal types of cells, however, were rarely found. Quantitatively, 57.60±1.67% (mean±S.D.) (371 of 693 cells) of anti-calretinin labeled neurons were round or oval, 19.30±1.26% (158 of 693 cells) were vertical fusiform, 19.10±1.28% (138 of 693 cells) were stellate, 2.04±1.08% (15 of 693 cells) were horizontal, and 1.80±1.07% (11 of 693 cells) were pyriform neurons (Fig. 9).

Although some cells were localized in the normal superficial layers, the staining was pale in most of the calretinin labeled neurons (Fig. 6). In the normal superficial SC, the morphology of labeled cells was similar to that of superficial layers of the SC contralateral to the enucleation. Figure 6D shows representative multipolar round or oval cells. Figure 6A shows a vertical fusiform cell, while Figure 6B shows a medium-sized stellate neuron. Figure 6C and 6E show rarely found pyriform and horizontal cells. Similar to labeled cells of the superficial layers of the SC contralateral to the enucleation, 51.30±1.35% (mean±S.D.) (74 of 144 cells) of anti-calretinin labeled neurons were round or oval, 20.81±0.52% (30 of 144 cells) were vertical fusiform, 18.73±0.60% (27 of 144 cells) were stellate, 5.00±0.43% (7 of 144 cells) were horizontal, and 4.16±0.48% (6 of 144 cells) were pyriform neurons in the normal superficial SC (Fig. 9).

The morphology of calretinin-IR neurons in the normal IGL and DGL was similar to that of the calretinin-IR neurons in the SGL. There were no systematic differences in the morphology of calretinin-IR neurons within the IGL and DGL among the normal, control, and experimental sides of the SC. The large majority of anti-calretinin-IR neurons were multipolar round or oval neurons in both the IGL and DGL (Figs. 7, 8). Figures 7A and 7B show typical vertical fusiform neurons in the IGL, while Fig. 7C and 7F show typical multipolar round or oval neurons. Stellate (Fig. 7E) and horizontal (Fig. 7G) neurons were also found. However, pyriform cells were not found in the IGL. Another noticeable feature of calretinin-IR neurons in the IGL was the presence of varicose dendrites. Figure 7D (arrowheads) shows a stellate neuron with varicose dendrites. Quantitatively, 55.35±1.29% (mean±S.D.) (212 of 383 cells) of anti-calretinin labeled neurons were round or oval, 21.67±0.50% (83 of 383 cells) were vertical fusiform, 20.62±0.48% (79 of 383 cells) were stellate, and 2.34±0.05% (9 of 383 cells) were horizontal neurons in the IGL (Fig. 9). Figure 8 shows representative calretinin-IR neurons in the DGL. Figures 8A and 8B show vertical fusiform neurons in the DGL, while Fig. 8C shows a multipolar round neuron. Figures 8D and 8E show multipolar stellate and horizontal neurons, respectively. Quantitatively, 46.82±0.71% (mean±S.D.) (118 of 252 cells) of anti-calretinin labeled neurons were round or oval, 25.39±0.38% (64 of 252 cells) were vertical fusiform, 24.60±0.37% (62 of 252 cells) were stellate, and 3.17±0.04% (8 of 252 cells) were horizontal neurons in the DGL (Fig. 9).

Co-localization of calretinin with GABA

To determine whether the calretinin-IR cells co-localize with GABA, we labeled calretinin with fluorescein and GABA with Cy5. We checked six sections of calretinin-IR neurons from two enucleated animals and six other sections of calretinin-IR neurons from two normal animals. We checked every calretinin-IR neuron within the superficial,

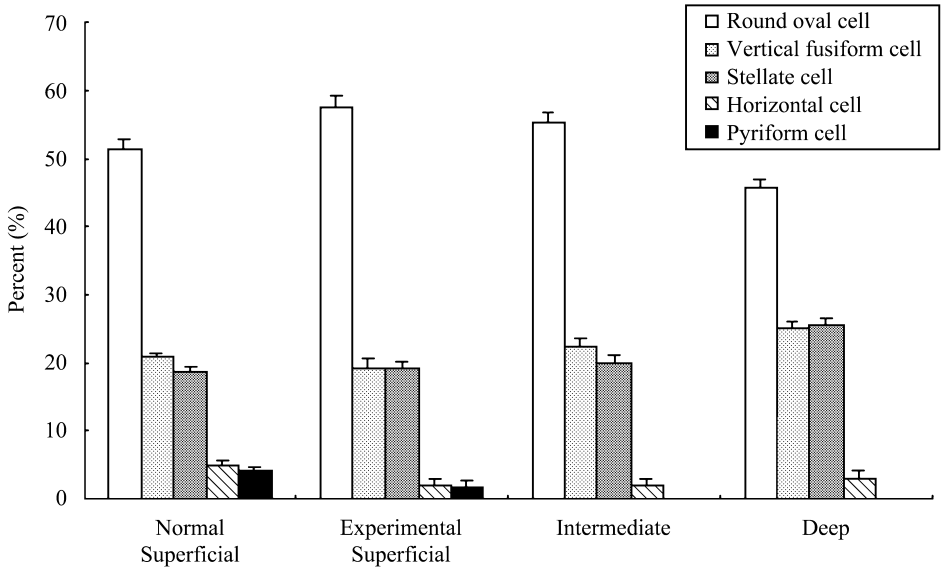

Fig. 9. Histogram of the distribution of calretinin-IR neurons in the dog SC. In all layers, the highest concentration of calretinin-IR neurons was multipolar round/oval neurons, while pyriform neurons were found only in the superficial layer. Note that the percentage of the labeled neurons in the superficial layers is similar both in the normal and experimental SC.

intermediate, and deep layers. Although some neurons with GABA or calretinin were similar in size, shape, and manner of the distribution in the superficial, intermediate, and deep layers, no neurons were labeled with both anti-calretinin and anti-GABA antibodies (Fig. 10).

Retrograde HRP tracing experiments

To further determine the subclass of retinal ganglion cells which supply calretinin-IR fibers for the SC, horseradish peroxidase (HRP) was used as a retrograde tracer to identify neurons in the retina. Among the six cases, HRP injections were successfully placed in the superficial SC in two cases. Among these two cases, many retrogradely labeled neurons were clearly observed in inferior retinal regions 13–16 mm away from the optic nerve head in one case. A small number of retrogradely labeled neurons were observed in the other case. Retinal whole mounts containing retrogradely labeled neurons were then treated for calretinin immunocytochemistry. Figure 11 shows the injection site that was concentrated in the superficial layer of the SC (Fig. 11D) of one animal that produced many retrogradely labeled ganglion cells with HRP and calretinin-labeled cells. Figure 11A shows a medium-sized calretinin-IR neuron (small arrowhead), a small HRP-labeled neuron (large arrowhead), and a small double-labeled neuron (arrow). Figure 11B shows small calretinin-IR neurons (small arrowheads) and small HRP-labeled neurons that also immunostained with calretinin (arrow). In this high power differential interference contrast photomicrograph, a large ganglion cell without calretinin was seen (asterisk). Figure 11C shows an HRP-labeled large ganglion cell along with a large ganglion cell none-IR for calretinin and a small ganglion cell IR for calretinin. We could find no double-labeled large (>30 μm) neurons in any areas of the retinal whole mounts in the present study. The vast majority of the double-labeled neurons (HRP and calretinin) were small (<15 μm).

IV. Discussion

The pattern of distribution of calretinin-IR fibers in the superficial layers of the dog SC is similar to that observed in previous studies in human [23], monkey [46], cat [13], rat [1], mouse [8], and hamster SC [21]; the antibody against calretinin formed a dense plexus of labeled fibers in the superficial layers of the SC. However, calretinin does not form a plexus of labeled fibers in the SGL of the rabbit SC. By contrast, many anti-calretinin-labeled neurons are localized in the superficial layers of the rabbit SC [20]. These results suggest that there are some species differences in calretinin immunoreactivity in the superficial layers of mammalian SC. This species diversity suggests that different functional needs respond best to different visual behavioral contexts and emphasizes the importance of the investigation of neurochemical architecture in diverse animals.

The present results in IGL indicate differences of the distributional pattern of calretinin-IR neurons that may reflect the functional differences of specific efferent and afferent connections of the SC across species. Leuba and Saini (1996) found a broad band of calretinin-IR neurons in the IGL and DGL in human. The distribution of calretinin-IR cells in the deeper layers of monkey SC also did not form any clusters [46]. In dog SC, the neurons in the IGL form clusters. Thus, important differences in calretinin distribution exist between human, monkeys, and dog SC. One of the most distinctive organizing characteristics of the SC is its compartmental architecture. Many efferent and afferent sys-

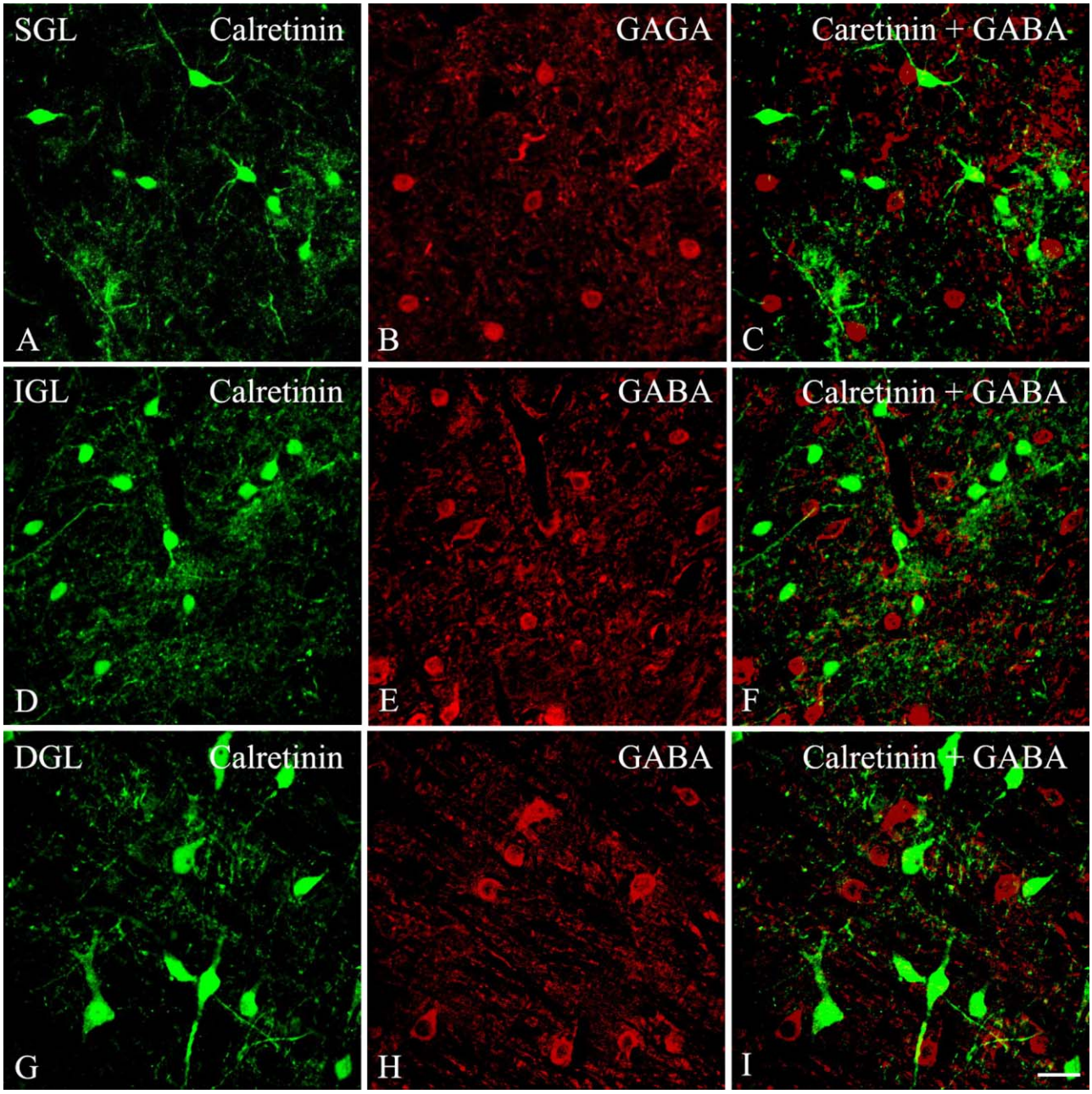

Fig. 10. Fluorescence confocal photomicrographs of dog SGL (upper), IGL (middle), and DGL (bottom) immunostained for calretinin (**A, D, G**) and GABA (**B, E, H**). (**C, F, I**) Superimposition of images in calretinin and GABA. Calretinin and GABA are expressed in different sets of neurons in the dog SC. Bar=20 μm.

tems show clusters, patches, puffs, or domains within the SC with spatially, neurochemically, and anatomically separated certain sensory and motor neurons [10, 15, 16, 26]. Quite precise modular organization of efferent cell clusters and afferent patches has also been reported in cat IGL; where the cell clusters that project to the cuneiform region were found to overlap precisely with the cholinergic terminal patches [18, 19]. The calretinin-IR clusters identified in the present study strongly suggest that they promote selective segregation of the information of collicular afferents for different classes of motor behavior.

The present results indicate that several types of calretinin-IR neurons are coexistent in the dog SC throughout the superficial, intermediate, and deep layers. In the present study, the calretinin-IR neurons in all layers of the dog SC were heterogeneous small-to medium-sized neurons including round/oval, vertical fusiform, stellate, and horizontal in shape. A few pyriform cells were also found in the superficial layers. However, we found no pyramidal cells in any layers of the SC. In contrast to our results, Leuba and Saini [23] found that calretinin-IR neurons in the human SC were small- to large-sized neurons including pyramidal-shaped

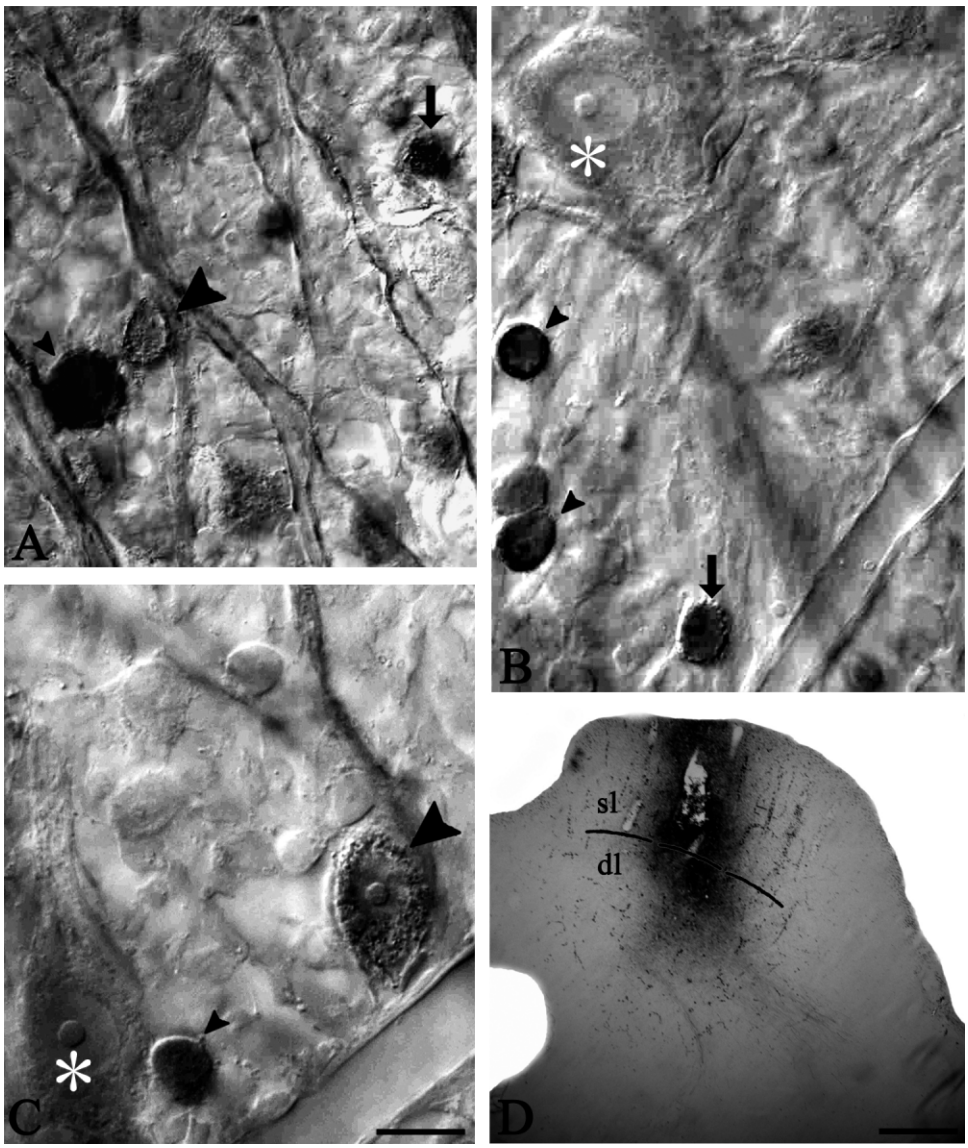

Fig. 11. Neurons single- or double-labeled by HRP and anti-calretinin antibody in a DAB-reacted whole mount of dog retina. HRP injections (30% HRP solution in distilled water) were made into the SC. The dogs were allowed to survive for 48 hr. (**A, B**) Higher magnification differential interference contrast photomicrograph showing some double-labeled cells (arrows), some single-labeled cells by HRP (large arrowheads), and an anti-calretinin antibody (small arrowheads). An unlabeled large retinal ganglion cell (asterisk) is seen in this differential interference contrast photomicrograph. (**C**) A large ganglion cell is labeled by HRP only (large arrowhead). An unlabeled large retinal ganglion cell (asterisk) and a single-labeled cell by calretinin are also seen in this differential interference contrast photomicrograph. (**D**) This photograph illustrates the density and size of HRP injection in the SC. sl, superficial layers; dl, deep layers. Bar=20 μm (**A–C**), 200 μm. (**D**).

cell bodies with a thick proximal dendrite oriented towards the pial surface. Monkey SC also contains numerous large calretinin-IR neurons in the IGL [25, 46]. In the present study, a unique class of calretinin-IR neurons was found in the dog IGL. These neurons had small cell bodies and distinctive varicose dendrites. Although these types of calretinin-IR neurons have not been described in other mammalian SC, such neurons have also been reported in calbindin-IR neurons in cat SC [32]. Whether these varicosities are related to vesicle containing dendrites can only be answered by electron microscopy. However, presynaptic density has been described in the IGL of the cat SC [36]. The present results combined with previous results indicate that there are differences in calretinin-IR neurons in mammalian SC. These differences in shape among different species indicate that the expression of calretinin gene in subclass of collicular neurons is different and reflect differences in their synaptic connections.

Similar to previous results [1, 8, 13, 21, 33, 47] in the current study a marked reduction in calretinin-immunoreactive fibers was produced in the superficial layers of the dog SC contralateral to the enucleation. Many calretinin-IR

neurons appeared in the superficial SC after enucleation. A number of researchers have suggested that calretinin is closely linked to activity-dependent changes. For example, unilateral cochlear ablation led to increased calretinin immunostaining within cochlear nucleus neurons [6]. The level of expression of calretinin in hippocampal neurons is tuned to the excitatory and inhibitory activity balance [27]. Enhanced stiatal excitatory input has been shown to increase the expression of calretinin in striatal neurons [34]. The present and previous results suggest that changes in the expression of calretinin occur in response to changes in neuronal activity. However, the current data showed that distributional patterns of morphological subtypes of calretinin-IR neurons in the superficial SC were similar between the normal and experimental sides. These results suggest that enucleation increases the expressional levels of mRNA that is expressed weakly in the normal state. Activity-dependent changes of calretinin mRNA have been reported [48]. Differentially to the superficial layers, however, enucleation appeared to have no effect on the calretinin-IR neurons in the intermediate and deep layers of dog SC. The present results suggest that the calretinin-containing neurons in superficial SC may be more plastic than calretinin-IR neurons in the intermediate and deep layers after enucleation.

Mammalian SC has been shown to contain a high concentration of GABAergic neurons [30, 37]. However, in the present study of two-color immunofluorescence demonstrated that there was no overlap between cells of which stained for calretinin and stained for GABA. These results suggest that calretinin-IR neurons are not GABAergic interneurons in the dog SC. Thus, the present results suggest that some of the calretinin-IR neurons in the dog SC are projection neurons. In contrast to the SC, large proportions of calretinin-IR neurons were found to be IR for GABA in the visual cortex [9, 28]. The quantitative data showing that the degree of colocalization of calretinin with GABA differs markedly in different visual structures indicate the unique chemical characteristics of calretinin.

In our previous HRP-tracer study in cat SC, we showed that the vast majority of calretinin-IR fibers in the superficial layers of the cat SC originate from small gamma-type cells that have W type physiologies [13]. Our current results show that the large retinal ganglion cells in the dog retina are negative against anti-calretinin immunoreactivity. The calretinin-IR fibers in the superficial dog SC were small. HRP injections in the superficial layers of the dog SC labeled both large and small retinal ganglion cells. However, none of the large ganglion cells were HRP and calretinin double-labeled. These results strongly suggest that calretinin-IR afferents in the superficial layers of the dog SC originate from small class retinal ganglion cells.

Although the biochemical properties of this protein have been well characterized, the functional properties of calretinin in the brain are still unclear. Suggested functions of calretinin comprise a role in neuroprotection against excitotoxicity or a calcium-buffering function in the cells expressing this protein in the brain [12, 40, 43]. A recent study has suggested that calretinin in the retinal ganglion cells plays an important role in optic nerve growth in the SC and in optic nerve regeneration after injury in zebra fish [7]. It may be possible that the clusters of the calretinin-IR neurons in the IGL receive input specifically related to eye movements [45]. There is also evidence that some saccade-related cells in the SC are organized into clusters [39]. Thus, calretinin may play a crucial role in saccadic eye movements. The many puffs and patches of multisensory afferents and motor efferents, the segregation and cluster of calretinin-IR neurons, and the heterogeneity of labeled neurons in the SC indicate a distinct role for calretinin in the SC. Our future investigations will seek to determine what the function is.

V. Acknowledgment

We thank Prof. Robert Flaherty, Language Institute of Kyungpook National University, for proofreading the English. This work was supported by a Grant (R01-2003-000-10505-0) from the Basic Research Program of the Korea Science and Engineering Foundation, and 2003 Kyungpook National University Research Team Fund.

VI. References

1. Arai, M., Arai, R., Sasamoto, K., Kani, K., Maeda, T., Deura, S. and Jacobowitz, D. M. (1993) Appearance of calretinin-immunoreactive neurons in the upper layers of the rat superior colliculus after eye enucleation. *Brain Res.* 613; 341–346.
2. Baimbridge, K. G., Celio, M. R. and Rogers, J. H. (1992) Calcium-binding proteins in the nervous system. *Trends Neurosci.* 15; 303–308.
3. Behan, M., Jourdain, A. and Bray, G. M. (1992) Calcium binding protein (calbindin D28k) immunoreactivity in the hamster superior colliculus: ultrastructure and lack of co-localization with GABA. *Exp. Brain Res.* 89; 115–124.
4. Celio, M. R. (1990) Calbindin D-28k and parvalbumin in the rat nervous system. *Neuroscience* 35; 375–475.
5. Cork, R. J., Baber, S. Z. and Mize, R. R. (1998) Calbindin D28k- and parvalbumin-immunoreactive neurons form complementary sublaminae in the rat superior colliculus. *J. Comp. Neurol.* 394; 205–217.
6. Fuentes-Santamaria, V., Alvarado, J. C., Taylor, A. R., Brunso-Bechtold, J. K. and Henkel, C. K. (2005) Quantitative changes in calretinin immunostaining in the cochlear nuclei after untilateral cochlear removal in young ferrets. *J. Comp. Neurol.* 483; 458–475.
7. Garcia-Crespo, D. and Vecino, E. (2004) Differential expression of calretinin in the developing and regenerating zebrafish visual system. *Histol. Histopathol.* 19; 1193–1199.
8. Gobersztejn, F. and Britto, L. R. G. (1996) Calretinin in the mouse superior colliculus originates from retinal ganglion cells. *Braz. J. Med. Biol. Res.* 29; 1507–1511.
9. Gonchar, Y. and Burkhalter, A. (1997) Three distinct families of GABAergic neurons in rat visual cortex. *Cereb. Cortex* 7; 347–358.
10. Harting, I., Blaschek, A., Wolf, N. I., Seitz, A., Haupt, M., Goebel, H. H., Rating, D., Sartor, K. and Ebinger, F. (2004) T2-hyperintense cerebellar cortex in Marinesco-Sjogren syndrome. *Neurology* 63; 2448–2449.
11. Heizmann, C. W., Röhrenbeck, J. and Kamphuis, W. (1990) Par-

valbumin, molecular and functional aspects. *Adv. Exp. Med. Biol.* 269; 57–66.
12. Heizmann, C. W. and Braun, K. (1995) Calcium Regulation by Calcium-binding Proteins in Neurodegenerative Disorders, Springer-Verlag, NY.
13. Hong, S.-K., Kim, J.-Y. and Jeon, C.-J. (2002) Immunocytochemical localization of calretinin in the superficial layers of the cat superior colliculus. *Neurosci. Res.* 44; 325–335.
14. Huerta, M. F. and Harting, J. K. (1984) The mammalian superior colliculus: studies of its morphology and connections. In "The Comparative Neurology of the Optic Tectum", ed. by H. Vanega, Plenum Press, New York, pp. 687–772.
15. Illing, R. B. and Graybiel, A. M. (1986) Complementary and non-matching afferent compartments in the cat's superior colliculus: innervation of the acetyl cholinesterase-poor domain of the intermediate gray layer. *Neuroscience* 18; 373–394.
16. Illing, R. B. (1992) Association of efferent neurons to the compartmental architecture of the superior colliculus. *Proc. Natl. Acad. Sci. U S A* 89; 10900–10904.
17. Illing, R. B. (1996) The mosaic architecture of the superior colliculus. *Prog. Brain Res.* 112; 17–34.
18. Jeon, C.-J. and Mize, R. R. (1993) Choline acetyltransferase-immunoreactive patches overlap specific efferent cell groups in the cat superior colliculus. *J. Comp. Neurol.* 337; 127–150.
19. Jeon, C.-J., Spencer, R. F. and Mize, R. R. (1993) Organization and synaptic connections of cholinergic fibers in the cat superior colliculus. *J. Comp. Neurol.* 333; 360–374.
20. Jeon, C.-J., Pyun, J.-K. and Yang, H.-W. (1998) Calretinin and calbindin D28K immunoreactivity in the superficial layers of the rabbit superior colliculus. *Neuroreport* 9; 3847–3852.
21. Kang, Y.-S., Park, W.-M., Lim, J.-K., Kim, S.-Y. and Jeon, C.-J. (2002) Changes of calretinin, calbindin D28K and parvalbumin immunoreactive neurons in the superficial layers of the hamster superior colliculus following monocular enucleation. *Neurosci. Lett.* 330; 104–108.
22. Lee, B.-C., Kim, M.-K., Jang, G., Oh, H.-J., Yuda, F., Kim, H. J., Shamim, M. H., Kim, J. J., Kang, S. K., Schatten, G. and Hwang, W. S. (2005) Dogs cloned from adult somatic cells. *Nature* 436; 641.
23. Leuba, G. and Saini, K. (1996) Calcium-binding proteins immunoreactivity in the human subcortical and cortical visual structures. *Vis. Neurosci.* 13; 997–1009.
24. Leuba, G., Kraftsik, R. and Sainin, K. (1998) Quantitative distribution of parvalbumin, calretinin, and calbindin D28K immunoreactive neurons in the visual cortex of normal and Alzheimer cases. *Exp. Neurol.* 152; 278–291.
25. Ma, T. P., Cheng, H. W., Czech, J. A. and Rafols, J. A. (1990) Intermediate and deep layers of the macaque superior colliculus: a Golgi study. *J. Comp. Neurol.* 295; 92–110.
26. Mana, S. and Chevalier, G. (2001) The fine organization of nigrocollicular channels with additional observations of their relationships with acetylcholinesterase in the rat. *Neuroscience* 106; 357–374.
27. Marty, S. and Onteniente, B. (1997) The expression pattern of somatostatin and calretinin by postnatal hippocampal interneurons is regulated by activity-dependent and -independent determinants. *Neuroscience* 80; 79–88.
28. Meskenaite, V. (1997) Calretinin-immunoreactive local circuit neurons in area 17 of the cynomolgus monkey, Macaca fascicularis. *J. Comp. Neurol.* 379; 113–132.
29. Mize, R. R., Jeon, C.-J., Butler, G. D., Luo, Q. and Emson, P. C. (1991) The calcium binding protein calbindin-D28K reveals subpopulations of projection and interneurons in the cat superior colliculus. *J. Comp. Neurol.* 307; 417–436.
30. Mize, R. R. (1992) The organization of GABAregic neurons in the mammalian superior colliculus. *Prog. Brain Res.* 90; 219–248.
31. Mize, R. R. and Luo, Q. (1992) Visual deprivation fails to reduce calbindin 28 kD or GABA immunoreactivity in the rhesus monkey superior colliculus. *Vis. Neurosci.* 9; 157–168.
32. Mize, R. R., Luo, Q., Butler, G., Jeon, C.-J. and Nabors, B. (1992) The calcium binding protein parvalbumin and calbindin-D28K form complementary patterns in the cat superior colliculus. *J. Comp. Neurol.* 320; 243–256.
33. Moschovakis, A. K., Karabelas, A. B. and Highstein, S. M. (1988) Structure-function relationships in the primate superior colliculus. I. morphological classification of efferent neurons. *J. Neurophysiol.* 60; 232–262.
34. Mura, A., Feldon, J. and Mintz, M. (2000) The expression of the calcium binding protein calretinin in the rat striatum: effects of dopamine depletion and L-DOPA treatment. *Exp. Neurol.* 164; 322–332.
35. Nabors, L. B. and Mize, R. R. (1991) A unique neuronal organization in the cat pretectum revealed by antibodies to the calcium-binding protein calbindin-D 28k. *J. Neurosci.* 11; 2460–2476.
36. Norita, M. (1980) Neurons and synaptic patterns in the deep layers of the superior colliculus of the cat. A Golgi and electron microscopic study. *J. Comp. Neurol.* 190; 29–48.
37. Okada, Y. (1992) The distribution and function of gamma-aminobutyric acid (GABA) in the superior colliculus. *Prog. Brain Res.* 90; 249–262.
38. Ostrander, E. A., Galibert, F. and Patterson, D. F. (2000) Canine genetics comes of age. *Trends Genet.* 16; 117–124.
39. Peck, C. K. (1984) Saccade-related neurons in cat superior colliculus: pandirectional movement cells with postsaccadic responses. *J. Neurophysiol.* 52; 1154–1168.
40. Polans, A., Baehr, W. and Palczewski, K. (1996) Turned on by Ca^{2+} The physiology and pathology of Ca^{2+}-binding proteins in the retina. *Trends Neurosci.* 19; 547–554.
41. Rogers, J., Khan, M. and Ellis, J. (1990) Calretinin and other calcium binding proteins in the nervous system. *Adv. Exp. Med. Biol.* 269; 195–203.
42. Rogers, J. H. and Resibois, A. (1992) Calretinin-D28k in the rat brain: Patterns of partial co-localization. *Neuroscience* 51; 843–865.
43. Schäfer, B. W. and Heizmann, C. W. (1996) The S100 family of EF-hand calcium-binding proteins: functions and pathology. *Trends Biochem. Sci.* 21; 134–140.
44. Schmidt-Kastner, R., Meller, D. and Eysel, U. T. (1992) Immunohistochemical changes of neuronal calcium-binding proteins parvalbumin and calbindin-D-28k following unilateral deafferentation in the rat visual system. *Exp. Neurol.* 117; 230–246.
45. Segraves, M. A. and Goldberg, M. E. (1987) Functional properties of corticotectal neurons in the monkey's frontal eye field. *J. Neurophysiol.* 58; 1387–1419.
46. Soares, J. G., Botelho, E. P. and Gattass, R. (2001) Distribution of calbindin, parvalbumin and calretinin in the lateral geniculate nucleus and superior colliculus in Cebus apella monkeys. *J. Chem. Neuroanat.* 22; 139–146.
47. Vugler, A. A. and Coffey, P. J. (2003) Loss of calretinin immunoreactive fibers in subcortical visual recipient structures of RCS dystrophic rat. *Exp. Neurol.* 184; 464–478.
48. Winsky, L. and Jacobowitz, D. M. (1995) Effects of unilateral cochlea ablation on the distribution of calretinin mRNA and immunoreactivity in the guinea pig ventral cochlear nucleus. *J. Comp. Neurol.* 354; 564–582.
49. Yang, F., O'Brien, P. C. M., Milne, B. S., Graphodatsky, A. S., Solanky, N., Trifonov, V., Rens, W., Sargan, D. and Ferguson-Smith, M. A. (1999) A complete comparative chromosome map for the dog, red fox, and human and its integration with canine genetic maps. *Genomics* 62; 189–202.
50. Yang, H.-W. and Jeon, C.-J. (1998) Distribution of calretinin in the superficial layers of the mouse superior colliculus: effect of monocular enucleation. *Korean J. Biol. Sci.* 2; 389–393.